Fusion Engineering and Design 121 (2017) 256–264

Contents lists available at ScienceDirect

Fusion Engineering and Design

journal homepage: www.elsevier.com/locate/fusengdes

Full Length Article

Discrete element modeling of pebble bed packing structures for HCCB TBM

Baoping Gong*, Yongjin Feng, Hongbin Liao, Yang Liu, Xiaoyu Wang, Kaiming Feng

Southwestern Institute of Physics, P.O. Box 432, Chengdu 610041, China

ARTICLE INFO

Keywords:
Packing structure
Packing factor
Pebble bed
Test blanket module
Discrete element method

ABSTRACT

In solid tritium breeder blanket, the tritium breeder and neutron multiplier are used in formed of pebbles. To reveal the inner packing structures of the pebble bed, in this paper, the discrete element method (DEM) was applied to simulate the pebble bed packing structures by pouring pebbles from the top of container. The current numerical results obviously show that with the increase of aspect ratios the packing factor can be significantly increased in both cylinder pebble bed and cubic pebble bed. Namely, the larger aspect ratios in cylinder and cubic pebble bed, the smaller the proportion of the wall affected region, the greater the average packing factor of the cylinder and cubic pebble bed. Furthermore, the pebble packing structures in a U-shaped container were also simulated and analyzed. In the bend pebble bed, the average packing factor of 0.6278 was obtained. Close to the convex and concave container wall, the wall effects of pebble distribution and packing factor were observed. With the increase of the distance to the container wall, the layered arrangements disappear gradually and the oscillating characteristics of local packing factor are also damped little by little. The oscillations of local packing factors are limited in about 5 diameters. A transition region is formed between the layered packing in the near wall region and the uniformly random packing in the inner bulk region. In addition, the contact force distribution and coordination number distribution were also detailed analyzed.

1. Introduction

In future fusion reactor, the tritium breeder blankets play a crucial role on the function of tritium self-sufficiency. ITER, as an international joint development program, will be used to demonstrate the scientific and engineering techniques of tritium breeding and tritium self-sufficiency. At present, several TBMs (Test Blanket Modules) for tritium producing, designed by each participant, will be tested on ITER. In China, CN HCCB TBM (Chinese Helium Cooled Ceramic Breeder Test Blanket Module) will be tested on ITER during different operation phases [1,2]. The packing factor γ, one of the key parameters for describing packing structure of pebble bed, affects the design of tritium breeder blanket. It also influences the effective thermal conductivity of pebble bed [3–7], the heat transfer coefficient of pebble-wall interface [7,8], the heat transfer throughout packed pebble bed [9,10], the thermal mechanical response [11–15], the flow characteristics of purge gas [16–22] and the tritium breeding ratio. So the packing factor is an important design parameter that must be known.

Many researchers have paid attention on the packing factor of pebble bed, which depends on lots of factors, such as the friction coefficient between pebbles and between wall and pebble [23], the pebble size and size distribution [24], the shape of container [25], the high of pebble bed and filling process [26–28]. In both square cavities and cylindrical containers, the pebble packing of glasses, beryllium, steel and lithium orthosilicate pebbles with different pebble size were investigated in [26,27]. The possible technologies of pebble packing process were explored under the TBM-relevant conditions of the EU HCPB TBM [28]. These experiment results show that vibrating pebble bed and tilting mock-up are effective approaches to obtain the dense packing, and the filling hole should be located at the highest position. Moreover, the x-ray 3D computer aided micro-tomography (CMT) allowing the reconstruction of 3D images within a pebble bed, and the Optical microscopy (OM) were applied to the investigations of inner structures and topological analysis of pebbles and pebble beds [29–35].

With the development of computer and numerical technologies, the numerical simulation is applied to investigate the behaviors of granular materials, progressively. The discrete element method (DEM) is a well numerical tool for modeling the realistic packing processes and the flow characteristics of granular materials [36]. The researchers have acquired lots of achievements by modeling pebble packing. The packing structures of random close packing in cylindrical container with mono-sized pebbles and in cubic region with binary-sized mixture pebbles were simulated respectively in [37]. And the packing in cylindrical cavities was compared with the experimental results by using x-ray tomography. Furthermore, the packing factor distribution in pebble bed reactors [23,38] and the packing structure of pebble bed for CFETR

* Corresponding author.
E-mail addresses: gongbp@swip.ac.cn, gongbp@gmail.com (B. Gong).

http://dx.doi.org/10.1016/j.fusengdes.2017.08.002
Received 3 January 2017; Received in revised form 28 June 2017; Accepted 1 August 2017

WCCB [39] was simulated by using DEM. However, the mostly simulations concentrate on the pebble packing in cubic, cylindrical and annular cavities. Thus the pebble packing in the U-shaped cavity of CN HCCB TBM still needs to be exploited.

In this study, the pebble packing structures in cylinder cavity and cubic container with different aspect ratios were simulated and analyzed for comparison with experimental results. In addition, the bend pebble bed in U-shaped container was focused by DEM. The packing structure, the packing factor distribution, contact force distribution and coordination number distribution of the bend pebble bed were detailed analyzed and compared with some experiment results.

2. Numerical modeling method and procedure

2.1. Discrete element method

Discrete element method is an effective numerical computation tool for investigating the micro-mechanisms of the granular systems, such as the lithium ceramic pebble bed and beryllium pebble bed of TBM. By DEM simulation lots of useful information can be easily obtained, some of which are difficult to measure from experiment. DEM is based on the Newton's Second Law of Motion, by which the movements and displacements of each particle are circularly calculated, and the physical contact theory of spherical particles, by which the contact forces with its neighbor particles are computed during the simulation. The contact force between two particles with very small overlap and the relation between force and deformation are determined according to Hertz-Mindlin contact theory [40,41]. During the DEM simulation process, each particle is treated as independent element. The movement of particle i is driven by the force balance showed in Eq. (1).

$$F_i = m_i g + \sum_j^n (\boldsymbol{F}_{nij} + \boldsymbol{F}_{tij}) = m_i g + \sum_j^n [(k_n \delta_{nij} - \eta_n v_{nij}) + (k_t \delta_{tij} - \eta_t v_{tij})]. \quad (1)$$

Where m is mass, g is gravity, n is neighbor number of particle i. $\boldsymbol{F}_{nij}$ and $\boldsymbol{F}_{tij}$ are the normal contact force and the tangential contact force between particle i and particle j. δ_{nij} is the overlap distance of particle i and j. δ_{tij} is tangential displacement vector between two particles. $\boldsymbol{v}_{nij}$ and $\boldsymbol{v}_{tij}$ are normal and tangential components of relative velocity between particle i and j. The elastic constant of normal and tangential contact are defined as follows

$$\boldsymbol{k}_n = \frac{4}{3}E^*\sqrt{R^*\delta_{nij}}, \quad \boldsymbol{k}_t = 8G^*\sqrt{R^*\delta_{nij}}. \quad (2)$$

The viscoelastic damping constant for normal and tangential contact are denoted respectively as

$$\eta_n = \sqrt{\frac{2}{3}}\alpha(2E^*\sqrt{R^*\delta n_{ij}}m^*)^{1/2}, \eta_t = \sqrt{\frac{2}{3}}\alpha(8G^*\sqrt{R^*\delta n_{ij}}m^*)^{1/2}. \quad (3)$$

Thus the relation of $\boldsymbol{k}_n$, $\boldsymbol{k}_t$ and η_n, η_t are separately as follows

$$\eta_n = \alpha\sqrt{\boldsymbol{k}_n{}^*m^*}, \quad \eta_t = \sqrt{2/3}{}^*\alpha^*\sqrt{\boldsymbol{k}_t{}^*m^*}. \quad (4)$$

where E^*, G^*, $R^*$and m^* are, respectively, the effective Young's modulus, effective shear modulus, the equivalent radius and effective mass. The α is relevant to the restitution coefficient e via $\alpha = -\frac{\sqrt{5}\ln e}{\sqrt{\ln^2 e + \pi^2}}$ [23]. The calculation of these effective properties can refer [42].

After calculating the force, the movement of particle i is calculated according to the Newton's Second Law of Motion. When the relation of the normal and tangential contact force satisfy the Coulomb Friction Law, the sliding motions will occur. At this time, $F_t \geq \mu|F_n|\cdot\frac{F_t}{|F_t|}$, where the μ is the rolling friction coefficient. The simulations in this work have been implemented in the open source DEM code LIGGGHTS [40,41].

Table 1
Mechanical physical properties of Li_4SiO_4 materials

Property	Symbol	Value(Li_4SiO_4)
Density (g/cm^3)	ρ	2.323
Young's modulus (GPa)	E	90
Poisson ratio	σ	0.24
Friction coefficient for pebble-pebble	μ	0.1
Friction coefficient for pebble-wall	μ	0.1

2.2. Pebble bed properties

In HCCB TBM, the tritium breeding region is filed with Li_4SiO_4 pebbles with 1 mm diameter. So in the view of Li_4SiO_4 pebble beds application in fusion blanket, the mechanical physical properties of Li_4SiO_4 materials were selected and used in this work (see Table 1). The Young's modulus of bulk Li_4SiO_4 materials has been measured in Refs. [43,44], and it depends on both temperature and porosity of materials. The relation is indicated as

$$E = 110(1-p)^3 \times [1 - 2.5 \times 10^{-4}(T - 293)] \ \text{(GPa)} \quad (5)$$

Where T is temperature in Kelvin and p is porosity of bulk material. For Li_4SiO_4 ceramic pebbles the porosity is about 5–6%. When temperature is about 20 °C, the Young's modulus is set as 90 GPa and the Poisson ratio is set as 0.24 [15,47]. Each pebble is assumed to spherical particle and the properties of pebbles are uniform. The fraction coefficient and the restitution coefficient for pebble-wall and for inter-pebbles are set as 0.1 and 0.5 due to the lack of experimental data and reference to literatures [15,47]. These Mechanical physical properties are comprehensively referenced from the Refs. [15,43–47].

2.3. Pebble packing procedure

In this study, Firstly, the effects of the aspect ratios, α, on the average packing factor is investigated. And to test and verify the validity of the method, the simulation results are compared with some experimental results coming from Refs. [9,21,48,49]. The aspect ratio of a cylindrical packed bed, $\alpha_{cylinder}$, is the ratio of cylinder diameter D to pebbles diameter d. For cubic packed bed, the aspect ratio, α_{cubic} is defined as the ratio of the length of bottom side of cubic container a to pebbles diameter d. Then we apply the DEM to simulate the pebble bed packing structures for HCCB TBM. In the solid tritium breeding blanket of HCCB TBM, The Li_4SiO_4 pebbles will be packed in the U-shaped container as shown in Fig. 1a [1,2]. Because of the high axial symmetry, the U-shaped container can be geometrically simplified as cuboid box and a bend column for the purpose of reducing computation. The pebble packing in box is similar to the packing in cubic container as analyzed in Section 3.1. So in this work, the pebble packing in a bend column container was simulated and analyzed. The dimensions of the bend column container were shown in Fig. 1b, and the height of the bend column pebble bed is 100 mm. Pebble diameter adopts 1 mm due to the diameters of Li_4SiO_4 pebbles are about 1 mm in concept design of CN HCCB TBM [1].

Generally, there are four packing modes for random packed pebble beds [50]: (a) Very Loose Random Packing (VLRP) formed by gradual defluidization of a fluidized bed or by sedimentation. (b) Random Loose Packing (RLP) obtained by rolling pebbles appropriately, or dropping pebbles into container to form a loose mass; (c) Random Poured Packing (RPP) obtained by pouring pebbles into container with an initial velocity. (d) Random Close Packing (RCP) obtained usually by vibrating packed bed [35]. In this study, the pebbles were inserted from top region of container and then packed inside a cubic geometry and a U-shaped bend column under the gravity, respectively. So the packing modes in this work belong to RPP.

Without the loss of the generally, the packing processes in these

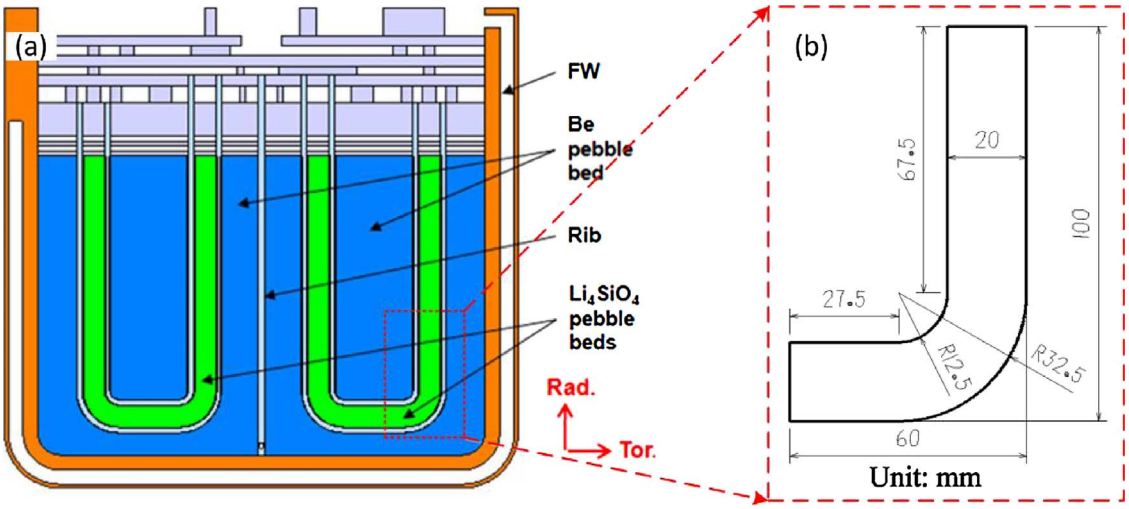

Fig. 1. Cross section of sub-module for HCCB-TBM and the dimensions of the bend column container.

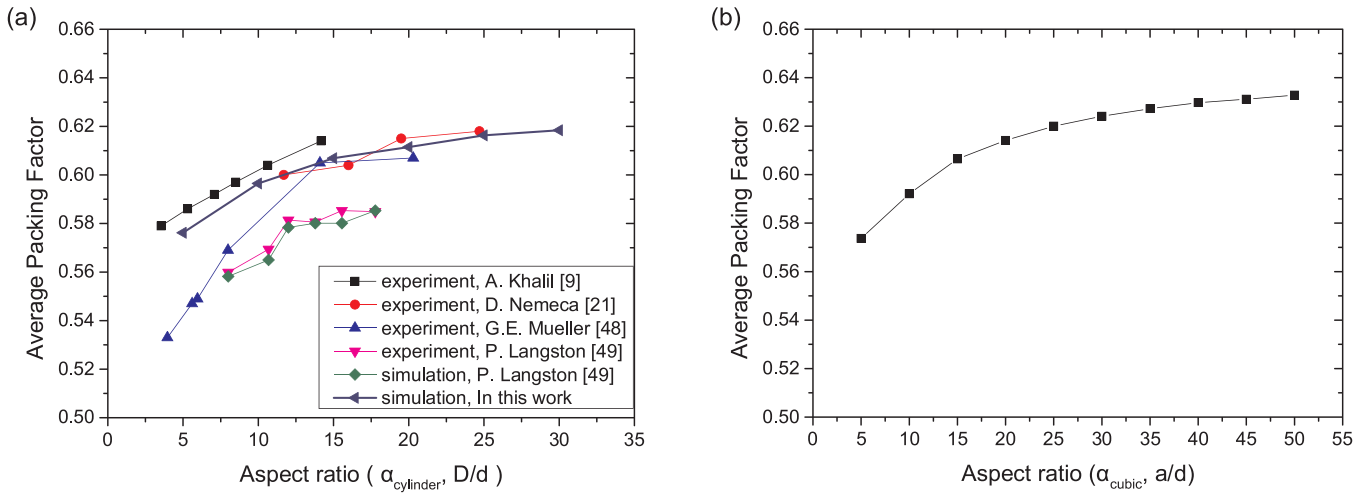

Fig. 2. Effects of the aspect ratios on average packing factor: a, cylinder pebble bed; b, cubic packed bed.

numerical experiments are as follow: Firstly, a certain number of pebbles were inserted in the top region of container with a very loose packing at inserting stage. Secondly, these pebbles with an initial velocity were free-falling after applying gravity at packing stage. Colliding and sliding appeared continuously and circularly during the packing process. At the same time, a variable number of pebbles would be reinserted in the top region every specified time-step. The numbers of pebbles in each reinsertion depend on both the maximum of inserting process and the pebbles still existed in the top region without falling down. That is because the reinserted pebbles cannot touch the existed ones for ensuring without larger overlap. The total numbers of pebble beds increased as time goes on. Thirdly, when the pebble beds reached specified height few particles were inserted any more. From that moment on the rearrangement did not stop until the pebbles reached the equilibrium state. Note that in this work the equilibrium state means that under the interaction of contact force and gravity, the net force and velocity of particles are close to zero owing to kinetic energy dissipation of pebbles during collision and sliding, and the particle positions (the center coordinates of pebbles) are almost no longer changing. In order to monitor the equilibrium state during the packing process, the translational kinetic energy and rotational kinetic energy were calculated every certain steps. Finally, all the pebbles randomly packed in the cavity. In this work, the total kinetic energy of pebble beds are about $\sim 10^{-14}$J and very close to zero in the end of these simulation. At this time the pebbles are approximated as neither rotating nor translating. The pebble bed can be considered to reach the equilibrium state and the packing structures are no longer changing.

3. Results and discussions

3.1. Effect of aspect ratios on packing factor

In the most previous researches, the attention to the effect of both container size and pebble size was focused on the aspect ratios in cylindrical pebble bed. And the majority region of the tritium breeding zone in HCCB TBM can be regarded as several long, tall, narrow cubic boxes and two bend columns. Thus, in this work, the effects of aspect ratios both in cylinder pebble bed and in cubic pebble bed were simulated and analyzed. The pebble diameters are all equal to 1 mm. Note that when calculating average packing factor, the pebble bed should be high enough and the region adjacent to bottom and top wall should be excluded for eliminating the wall effects of bottom and top wall.

The effects of the aspect ratios of cylindrical pebble bed were studied and compared with the experimental results referred to literature [9,21,48,49], in Fig. 2a. These results obtained in this work are in good accord with the previous experiment results [9,21,48,49]. All these results showed the same trend that the packing factor increased with the growing of the aspect ratios, $\alpha_{cylinder}$. The average packing factors increased from 0.5762 with $\alpha_{cylinder}$ = 5 to 0.6184 with $\alpha_{cylinder}$ = 30.

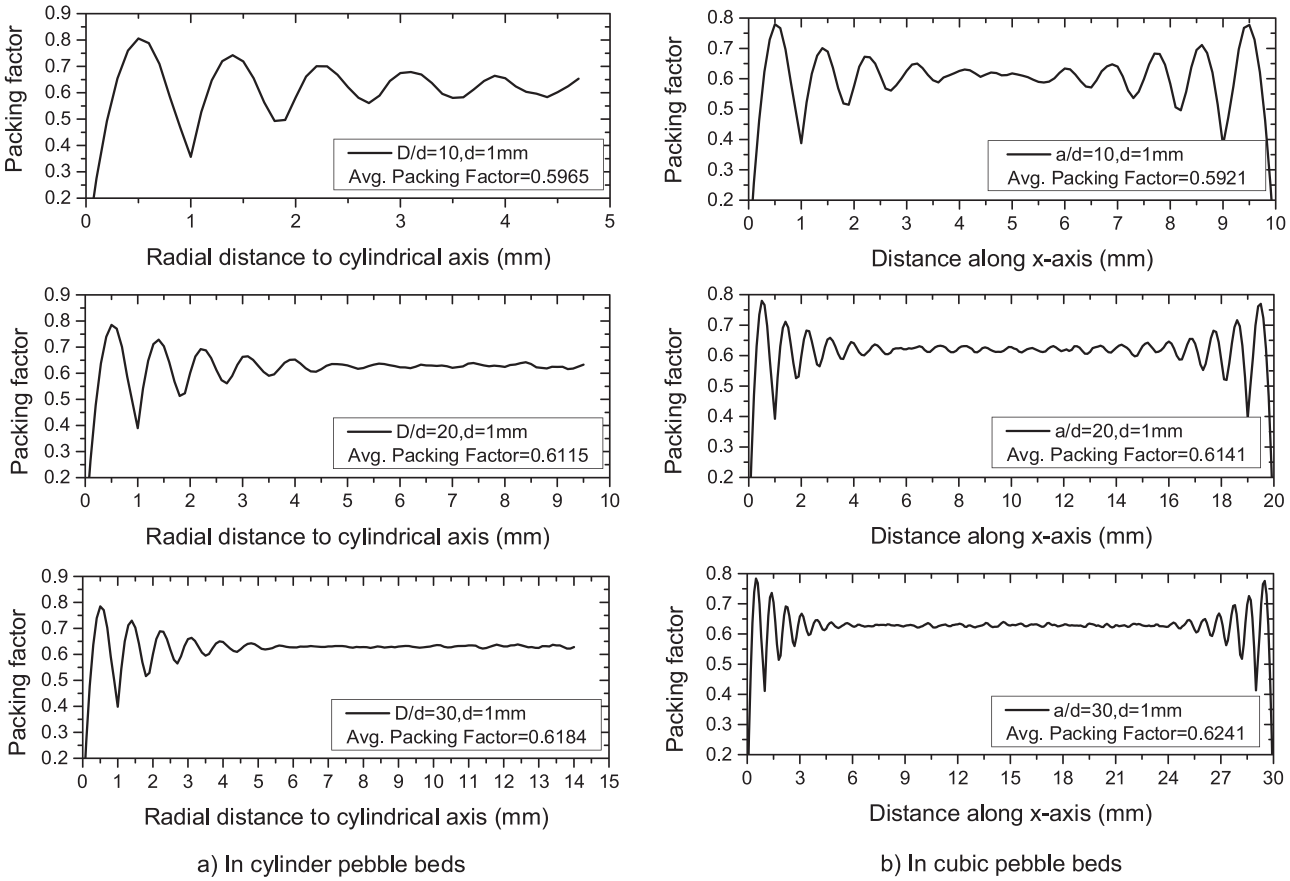

Fig. 3. Packing factor distribution in cylinder pebble bed (a) and cubic pebble bed (b).

The effects of the aspect ratios in cubic pebble bed, however, are few revealed in literature. So the pebbles packed in the cubic containers with the various aspect ratios, α_{cubic}, were also simulated in this work. The results are shown in Fig. 2b. It is clearly show that the packing factors in cubic pebble bed also increase with the increase of the aspect ratios α_{cubic} of cubic pebble bed. When the aspect ratios α_{cubic} are 5 and 50, the average packing factors are equal to 0.5737 and 0.6328, respectively. In contrast $\alpha_{cubic} = 5$, the average packing factor increased by 10.3% when $\alpha_{cubic} = 50$.

The trends, average packing factor increasing with the growing aspect ratios, are partly attributed to the effects of container walls. The Fig. 3 provides figures of packing factor distribution in mono-sized cylinder and cubic pebble bed. In cylinder pebble bed, the packing factors are drastic fluctuation throughout the pebble bed when $\alpha_{cylinder}$ is 5. And when aspect ratio $\alpha_{cylinder}$ is equal to 50, the packing factor shown a fluctuation with the decrease of the amplitude along the increasing of distance to container wall. The fluctuation is limited in about 5 pebble diameters close to container wall. In the inner region, the packing factor gradually reached a stable value, namely the average packing factor. Due to the wall effect, the local average packing factors in the near wall region and corner region have smaller values [35]. Compared with the whole pebble bed, the volume fractions of wall effect regions are gradually declined with the growth of aspect ratios. Thus the packing factors increase with the growing of the aspect ratios of $\alpha_{cylinder}$. Similar characteristics were observed in the cubic pebble beds. To sum up, the larger the aspect ratios in cylinder and cubic pebble bed, the smaller the proportion of the wall affected region, the greater the average packing factor of the cylinder and cubic pebble bed.

3.2. Packing structures of U-shaped pebble bed

3.2.1. 3D packing structures

The ceramic tritium breeder materials are used in the form of pebbles and packed in the U-shaped containers [1,2]. In this section, the pebble packing structure in a bend column container was simulated and analyzed. The dimensions of the bend container were shown in Fig. 1b, and the height of the bend pebble bed is 100 mm. Pebble diameter adopts 1 mm due to the diameters of Li_4SiO_4 pebbles are about 1 mm in concept design of CN HCCB TBM [1]. Other material parameters in Table 1 are employed in this simulation. With the help of ParaView [51], a visualization method has been applied to visualize the pebble bed from DEM simulation results.

Fig. 4 shows the 3D views of the pebble bed packing structures for mono-sized bend pebble bed in the equilibrium state. In Fig. 4a, the pebbles were colored by the unbalanced force of each pebble. The unbalanced force is the net forces on pebbles including the gravity and contact forces. The average unbalanced force in the pebble bed is about 7.26×10^{-11} N. In Fig. 4b, the pebbles were colored by the velocities of pebbles. The average velocity of pebbles in the bend pebble bed is about 2.50×10^{-8} m/s. Owing to such small velocity and unbalanced force, the movements of the pebbles are very small and the positions of the pebbles are almost constant. At this moment the packing structure of the bend pebble bed can be considered as stable state and can be further analyzed. There are 308,083 pebbles in the bend pebble bed at the final equilibrium state.

To reveal the inner packing structure, the pebble centers of the bend pebble bed at final equilibrium state were projected to the bottom plane, namely X-Y plane, as shown in Fig. 5a. To clearly show the detail internal structures of the bend pebble bed, the local views in the rectangle region and the local bend region were enlarged and figured in Fig. 5b–d. The points represent the pebble centers. It can be seen that in

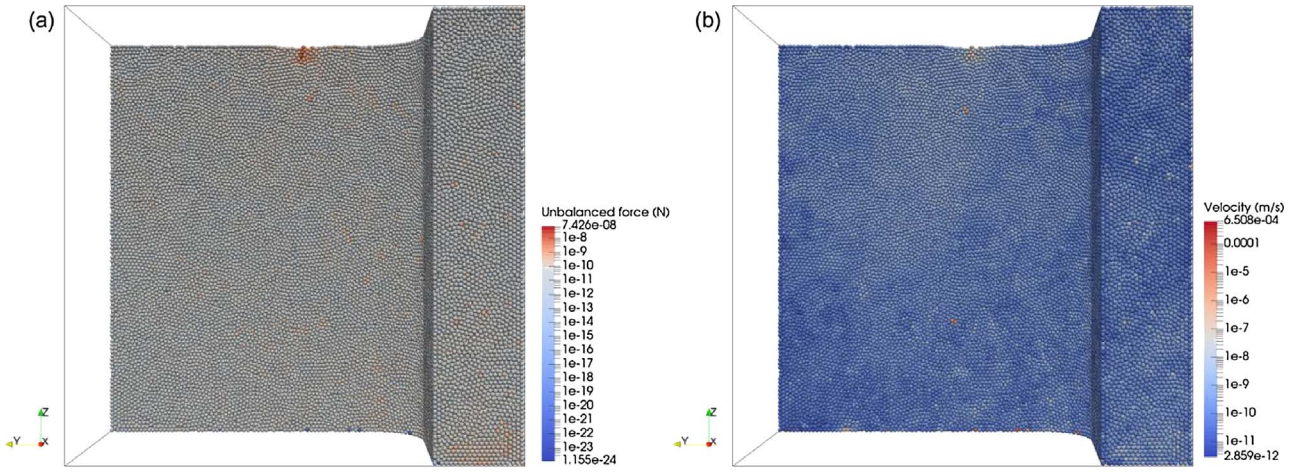

Fig. 4. 3D visualization of U-shaped pebble bed colored by (a) unbalanced force and (b) velocity (color online).

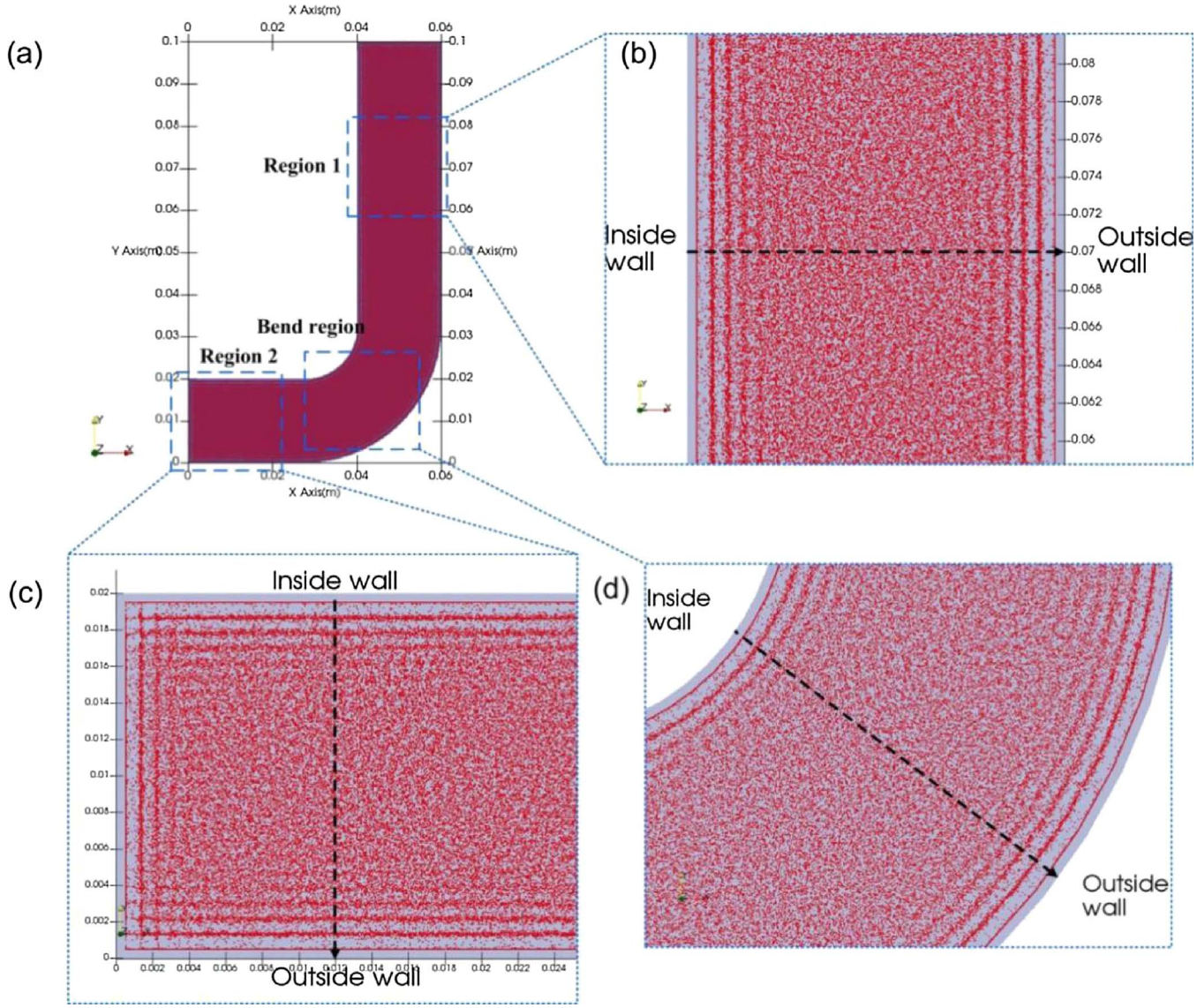

Fig. 5. Pebble center distribution of U-shaped pebble bed (color online).

the near wall region, the pebble centers packed and formed some regular layers. While in the inner bulk region, the pebble centers distributed uniformly and randomly. With the increase of distance to the container wall the layered arrangements disappeared gradually. A transition region was formed between the layered region and the inner bulk region. Close to the straight wall, about 4 layers were formed. Near the outside concave wall, there are about 4–5 layers. While close to the inside convex wall, only 3–4 layers were formed. In the straight corner region the layers intersected and formed mesh structure. These layered and meshed characteristics of pebble center distribution may form the relatively regular and loose packing structures and cause the packing factor variation. The packing factor distributions in the bend pebble bed will be analyzed in the following section.

3.2.2. Packing factor distribution

The packing factor is an important parameter to reveal the packing structure of a pebble bed, which is affected by many factors, such as the pebble size and the size distribution, the shape of pebbles, the dimension of container, the packing process, and so on. The average packing factor is defined by the volume ratio of solid pebbles to the whole pebble bed. To calculate the local packing factor, a method, proposed by Mueller [52], is used in this study. The pebble bed is divided into many parallel layers by many parallel cutting walls. As the thicknesses of these layers approaching zero, the local packing factor is determined by the area ratio of the summed intersection areas between all pebbles and the cutting wall to the cross areas of the parallel layers. And in the bend region the cutting walls are 1/4 cylindrical walls with the same center axis. Note that when calculating the local packing factor close to container wall, such as bottom wall, the regions close to other walls, such as side walls, should be excluded for excluding the influences of other container wall.

The average packing factor of the bend pebble bed is 0.6278. The local packing factor distributions are figured in Fig. 6. The variations of the local packing factors correspond to the pebble center distributions showed in Fig. 5. The radial local packing factor along the arrows in the rectangle region and the bend region shown in Fig. 5 are calculated and figured in Fig. 6a. It can be seen that close to the inside convex wall and the outside concave wall of the bend region, the pebbles obviously arranged several regular layers, especially at the line that adjoined to container wall and formed by the first layer pebble centers, which will result in a peak value of local packing factor as shown in Fig. 6a. While in the region between the neighbor layers, namely the region with sparse pebble centers, a nadir value of local packing factor was observed. With the increase of the distance to the container wall the layered arrangements disappeared gradually and the oscillating characteristics of local packing factor also damped little by little. The oscillations of local packing factors were all limited in about 5 diameters distance to container wall. A transition region was formed between the layered region and the inner bulk region. The layered arrangements and the transition region will result in the oscillatory and damped behavior of local packing factor with the increase of the distance to container wall. It is the so-called wall effect, which is a typical characteristic of granular system. In the inner bulk region, however, the pebble centers distributed uniformly and randomly. And the local packing factor also reached a stable value, namely the average packing factor of the inner bulk region.

The Fig. 6b shows the local packing factor of the bend pebble bed as a function of the distance to the bottom wall. The local packing factors also oscillated and damped in the near bottom wall region. The oscillation is limited in about 4.5 pebble diameters and the oscillating period is about 0.9 pebble diameters. A similar characteristic of bottom wall effect was observed as shown in Fig. 6d. Compared with the results in literature, the simulation results in this work are in a good agreement with the experimental results carried out by Klerk [50], which indicates that the pebble bed obtained in this DEM simulation has a reasonable and typical packing structure.

Noticeable, the oscillating and damping characteristics of the local packing factor reveal that the flow characteristics of purge gas and thermal exchange between pebble bed and structure materials may be influenced. And the researches about the influence of wall effect on flow characteristics are ongoing.

3.2.3. Contact force distribution

Force chains that are formed by mechanical contacts of inter-particles play an important role in pebble bed. The net-shaped framework formed by force chains supports the whole pebble bed. The strong force chains of pebble bed carry the majority of stress and external load. The low force chains, throughout the whole pebble bed, keep the stability of the pebble bed packing structure. Furthermore, the force chains are helpful in understanding the heat transfer mechanism of pebble bed, such as the Li_4SiO_4 pebble bed and the beryllium pebble bed of HCCB TBM. The pathways, formed by force chains, have a smaller resistance to the heat transfer for the pebble bed with high ratio of solid to gas thermal conductivity, especially. The force chains, colored by contact forces, of the bend pebble bed were displayed in Fig. 7. And the color represents the magnitude of contact force. The unit of contact force is N. To illustrate the details, the partial views in the top, middle, bottom region were amplified in Fig. 5, respectively. It can be seen that with the increase of the pebble bed height, the strength of the contact force chains are gradually weakened. There is a strong contact force chain between pebbles in the bottom region, while the contact force between the top region particles is relatively weak. The phenomenon mainly

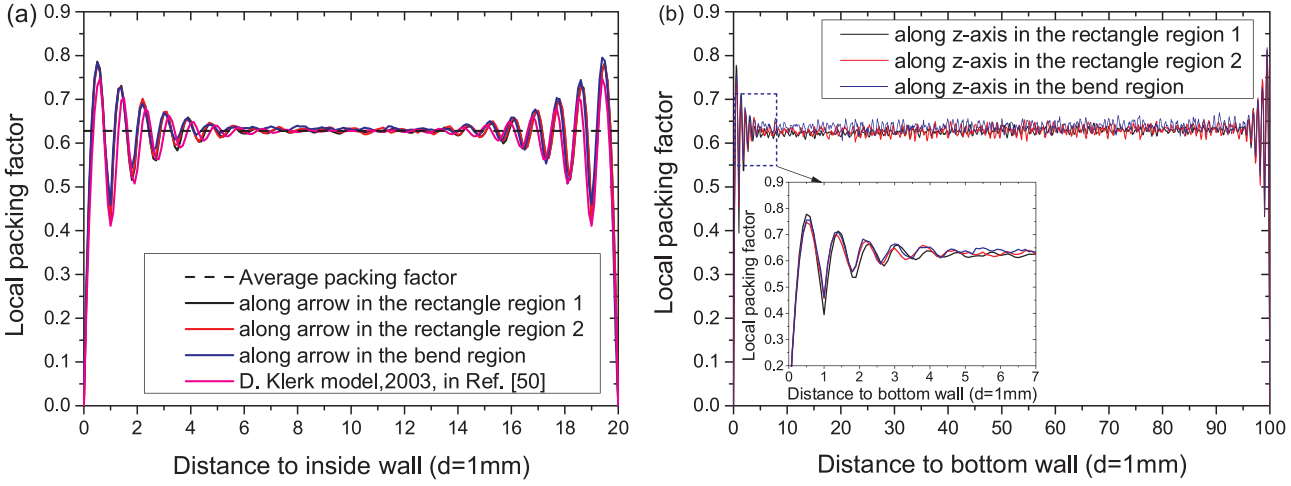

Fig. 6. Packing factors distribution. (a) Along the distance to inner wall; (b) Along the distance to bottom wall (color online).

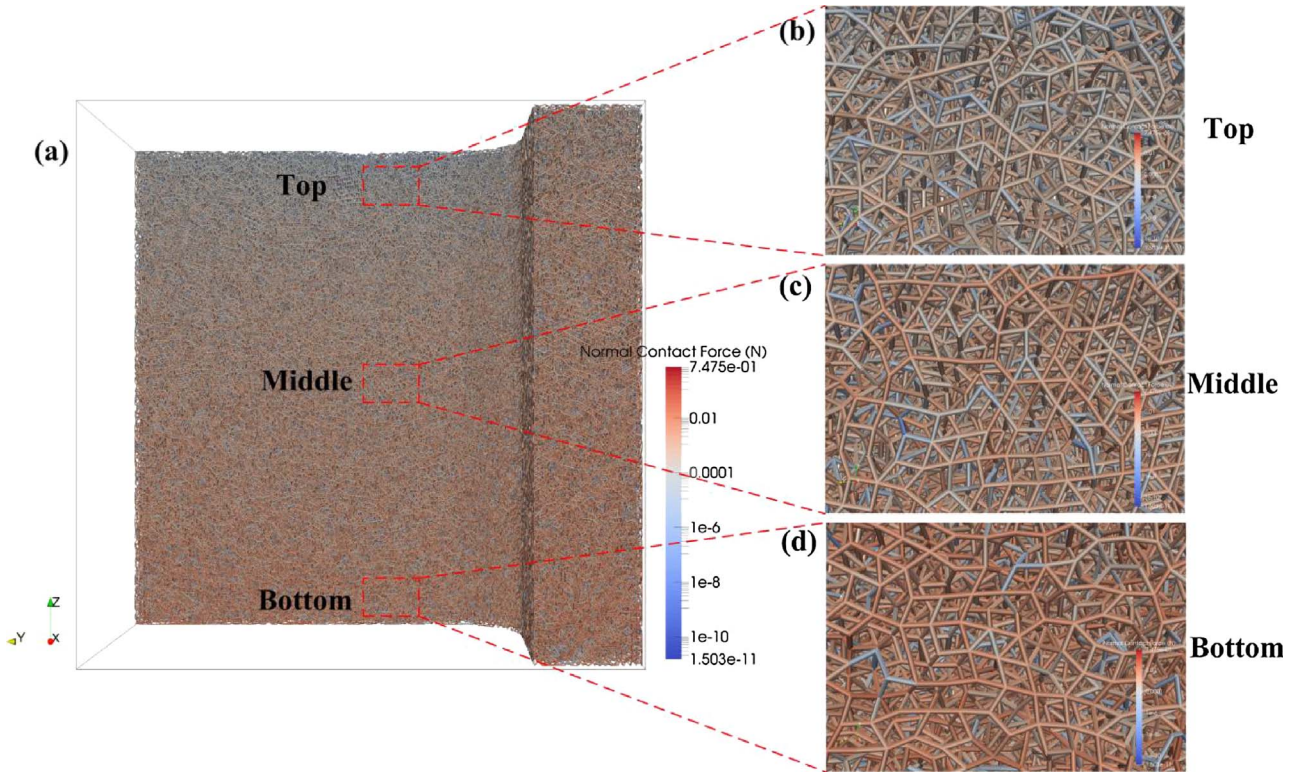

Fig. 7. Normal contact force chain of U-shaped pebble bed (color online).

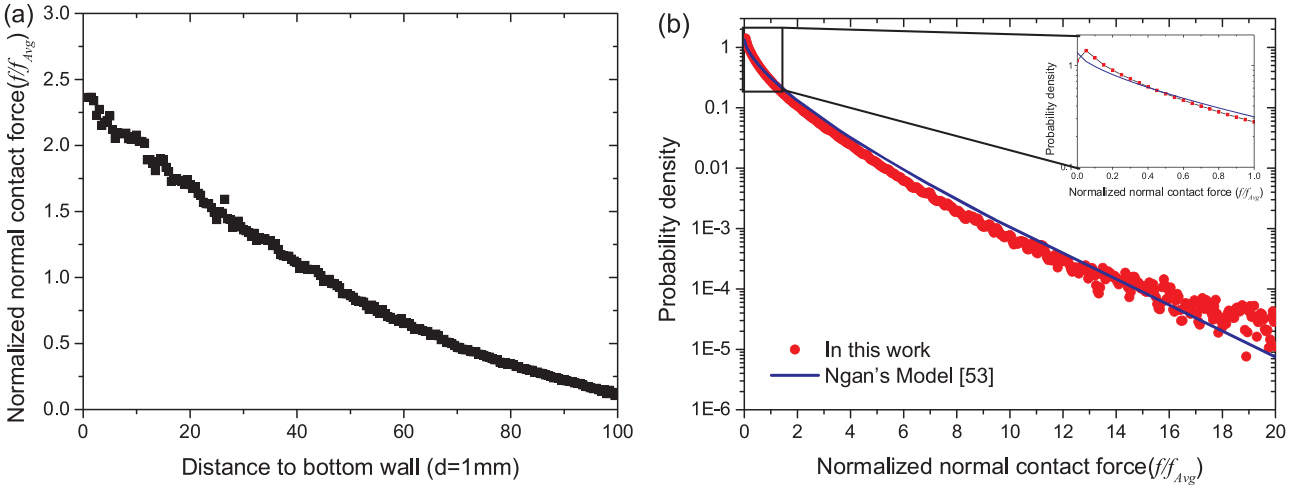

Fig. 8. Normal contact force distribution of U-shaped pebble bed: a, Position distributions; b, Probability distributions.

stems from the fact that the gravity was applied to each pebble during the packing process. A greater contact force between the particles in the bottom region can counteract the greater pressure exerted by the upper particles due to the gravity. Thereby the entire pebble bed can reach a stable packing state.

The contact force distributions, the position distribution and the probability distribution, are the most typical characterization of contact force chains. The position distribution of contact forces along the Z-axis in mono-sized bend pebble bed is plotted in Fig. 8a. Here, the f/f_{avg} is the normalized contact forces and the f_{avg} indicates the average contact force over whole pebble bed. Note that in this simulation the mechanical compaction wasn't applied on the bend pebble bed. The average normalized contact forces have no distinct trend profiles along X-axis and Y-axis and just oscillate around the average contact forces. Along the Z-axis, the average normalized contact forces decrease with the increase of bed height due to the effect of gravity, which are in agreement well with the physical phenomenon. Thus, the pebbles in the bottom region are more likely to be crushed.

Based on the statistical analysis, the probability distribution of normalized contact forces in the bend pebble bed is shown in Fig. 8b. The probability density first climb up slightly and then decline rapidly when the normalized contact force near zero. The distributions of normalized contact forces in the mono-sized bend pebble bed at equilibrium state are in agreement well with the Ngan's Model [53].

3.2.4. Coordination number distribution

Coordination number is an important micro parameter to characterize a granular system. It is determined by the number of the pebbles in contact with a certain pebble. To compare to the coordination number in experiments, the cut-off distance was set to 1.005

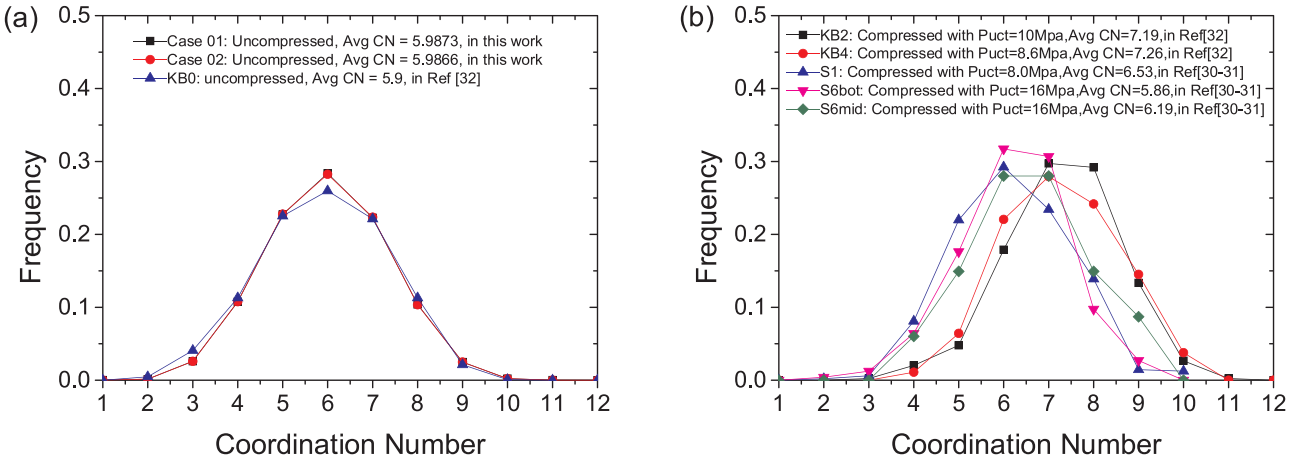

Fig. 9. Coordination number distributions of mono-sized pebble bed: a, uncompressed pebble beds; b, compressed pebble beds.

diameters for searching neighboring pebbles and calculating coordination number. If the distance between two pebble centers less than the cut-off distance, these two pebbles are considered to be in contact. The frequency distributions of coordination number in the bend pebble bed with two simulation cases are plotted and compared with experimental results of uncompressed pebble bed [32] in Fig. 9a. The same simulation conditions were applied to these two cases. There are 308,083 and 308,392 pebbles in the bend pebble bed of case01 and case02 respectively. It can be seen that there is no significant difference in the coordination number distributions of these two pebble beds. The coordination number of the bend pebble bed is changed in the region of 2–12. The average coordination number is 5.9873 and 5.9866 in the mono-sized pebble bed of case01 and case02 respectively. The most probable values are 6 in uncompressed mono-sized pebble bed, which is obviously comparable to the experimental results reported in Ref. [32], the average coordination number is 5.9 in KB0 [30,31]. Besides, the coordination number distributions of compressed pebble beds, which are from Refs. [30,31], are plotted in Fig. 9b. The maximum values of coordination number are between 6 and 7. Compared to uncompressed pebble bed, the pebbles in compressed mono-sized pebble bed have more contact.

4. Conclusion

DEM was applied to simulate the pebble packing behaviors of mono-sized pebble bed in cubic and a bend column container, respectively, by pouring pebbles into the container. It is demonstrated that the DEM code can well simulate the reasonably and realistically pebble packing process. And the DEM simulation can provide more useful information about the pebble packing structures of pebble bed.

From the results obtained in this study, it is clearly that with the augment of the aspect ratios, the increase of average packing factor are observed both in cubic and cylindrical pebble bed. The results in this work were obviously comparable to the experimental results. Further, the pebble packing structures in a bend column pebble bed, which was simplified from U-shaped containers of HCCB TBM, was analyzed. The result gives more information about the packing structure of pebble bed. Especially in the near wall region, the oscillating and damping characteristics of local packing factors were observed. In addition, the contact force and coordination number distributions were detailed analyzed.

Acknowledgments

This work was supported by the Chinese National Special Project for Magnetic Confined Nuclear Fusion Energy from Ministry of Science and Technology of China with grant numbers 2013GB108001 and 2014GB111001.

References

[1] K.M. Feng, G.S. Zhang, G. Hu, et al., New progress on design and R & D for solid breeder test blanket module in China, Fusion Eng. Des. 89 (2014) 1119–1125.
[2] K.M. Feng, X.Y. Wang, Y.J. Feng, et al., Current progress of Chinese HCCB TBM program, Fusion Eng. Des. 109–111 (2016) 729–735.
[3] D. Mandal, D. Sathiyamoorthy, M. Vinjamur, Experimental measurement of effective thermal conductivity of packed lithium-titanate pebble bed, Fusion Eng. Des. 87 (2012) 67–76.
[4] D. Mandal, D. Sathiyamoorthy, M. Vinjamur, Void fraction and effective thermal conductivity of binary particulate bed, Fusion Eng. Des. 88 (2013) 216–225.
[5] Zhou Zhao, K.M. Feng, Y.J. Feng, Theoretical calculation and analysis modeling for the effective thermal conductivity of Li_4SiO_4 pebble bed, Fusion Eng. Des. 85 (2010) 1975–1980.
[6] L. Chen, Y. Chen, K. Huang, et al., Investigation of effective thermal conductivity for pebble beds by one-way coupled CFD-DEM method for CFETR WCCB, Fusion Eng. Des. 106 (2016) 1–8.
[7] L. Chen, Y. Chen, K. Huang, et al., Effective thermal property estimation of unitary pebble beds based on a CFD-DEM coupled method for a fusion blanket, Plasma Sci. Technol. 17 (12) (2015) 1083–1087.
[8] Y. Gan, M. Kamlah, Thermo-mechanical modelling of pebble bed-wall interfaces, Fusion Eng. Des. 85 (2010) 24–32.
[9] A. Khalil, M.A. Kassem, M. Salama, Experimental evaluation of packed bed heat transfer relations, J. Eng. Comput. Sci. Qassim Univ. 1 (January (1)) (2008) 43–55.
[10] T. Tsory, N. Ben-Jacob, T. Brosh, et al., Thermal DEM-CFD modeling and simulation of heat transfer through packed bed, Powder Technol. 244 (2013) 52–60.
[11] Z. An, A. Ying, M. Abdou, Numerical characterization of thermo-mechanical performance of breeder pebble beds, J. Nucl. Mater. 367–370 (2007) 1393–1397.
[12] A. Ying, J. Reimann, L. Boccaccini, et al., Status of ceramic breeder pebble bed thermo-mechanics R & D and impact on breeder material mechanical strength, Fusion Eng. Des. 87 (2012) 1130–1137.
[13] Z. An, A. Ying, M. Abdou, Experimental & numerical study of ceramic breeder pebble bed thermal deformation behavior, Fusion Sci. Technol. 47 (2005) 1101–1105.
[14] D. Aquaro, N. Zaccari, Pebble bed thermal-mechanical theoretical model application at the geometry of test blanket module of ITER-FEAT nuclear fusion reactor, Fusion Eng. Des. 75-79 (2005) 903–909.
[15] X. Wang, M. Ye, H. Chen, Computational study on the behaviors of granular materials under mechanical cycling, J. Appl. Phys. 118 (2015) 174901.
[16] A. Abou-Sena, F. Arbeiter, L.V. Boccaccini, et al., Experimental study and analysis of the purge gas pressure drop across the pebble beds for the fusion HCPB blanket, Fusion Eng. Des. 88 (2013) 243–247.
[17] T. Eppinger, K. Seidler, M. Kraume, DEM-CFD simulation of fixed bed reactors with small tube to particle diameter ratios, Chem. Eng. J. 166 (2011) 324–331.
[18] T. Atmakidis, E.Y. Kenig, CFD-base analysis of the wall effect on the pressure drop in packed beds with moderatre tube/particle diameter ratios in the laminar flow regime, Chem. Eng. J. 155 (2009) 404–410.
[19] A. Montillet, E. Akkari, J. Comiti, About a correlating equation for predicting pressure drops through packed beds of spheres in a large range of Reynolds numbers, Chem. Eng. Process. 46 (2007) 329–333.
[20] A.M. Ribeiro, P. Neto, C. Pinho, Mean porosity and pressure drop measurements in packed beds of monosized spheres: side wall effects, IRECHE 1 (1) (2010) 40–46.
[21] N. Damjan, J. Levec, Flow through packed bed reactors:1. Single-phase flow, Chem. Eng. Sci. 60 (2005) 6947–6957.
[22] H. Zhang, H. Guo, H. Huang, et al., Numerical analysis of bypass flow in ceramic pebble beds, J. Fusion Energy 35 (2016) 385–389.
[23] H. Suikkanen, J. Ritvanen, P. Jalali, et al., Discrete element modelling of pebble packing in pebble bed reactors, Nucl. Eng. Des. 273 (2014) 24–32.

[24] Y. Shi, Y. Zhang, Simulation of random packing of spherical particles with different size distributions, Appl. Phys. A 92 (2008) 621–626.
[25] Y. Li, N. Gui, X. Yang, et al., Effect of wall structure on pebble stagnation behavior in pebble bed reactor, Ann. Nucl. Energy 80 (2015) 195–202.
[26] J. Reimann, A. Abou-Sena, R. Nippen, et al., Pebble bed packing in square cavities, KIT Scientific Report 7631, Karlsruhe Institute of Technology, 2012.
[27] J. Reimann, A. Abou-Sena, R. Nippen, et al., Pebble bed packing in prismatic containers, Fusion Eng. Des. 88 (2013) 2343–2347.
[28] A. Abou-Sena, H. Neuberger, T. Ihli, Experimental investigation on possible techniques of pebbles packing for the HCPB test blanket module, Fusion Eng. Des. 84 (2009) 355–358.
[29] F. Scaffidi-Argentina, G. Piazza, A. Goraieb, et al., Non destruction three dimensional analysis of the packing of a binary beryllium pebble bed, Fusion Eng. Des. 58–59 (2001) 707–712.
[30] R.A. J.Reimann, M.D. Pieritz, Michiel, et al., Inner structures of compressed pebble beds determined by X-ray tomography, Fusion Eng. Des. 75–79 (2005) 1049–1053.
[31] J. Reimann, R.A. Pieritz, R. Rolli, Topology of compressed pebble beds, Fusion Eng. Des. 81 (2006) 653–658.
[32] J. Reimann, E. Brun, C. Ferrero, et al., X-ray tomography investigation on pebble bed structures, Fusion Eng. Des. 83 (2008) 1326–1330.
[33] R.A. Pieritz, J. Reimann, C. Ferrero, 3D tomography analysis of the inner structure of pebbles and pebble beds, Adv. Eng. Mater. 13 (3) (2011) 145–155.
[34] M. Suzuki, T. Shinmura, K. Iimura, et al., Study of the wall effect on particle packing structure using X-ray micro computed tomography, Adv. Powder Technol. 19 (2008) 183–195.
[35] J. Reimann, E. Brun, C. Ferrero, et al., Pebble bed structures in the vicinity of concave and convex walls, Fusion Eng. Des. 98–99 (2015) 1855–1858.
[36] P.A. Cundall, O.D.L. Starck, A discrete numerical model for granular assemblies, Geotechnique 29 (1) (1979) 47–65.
[37] Y. Gan, M. Kamlah, J. Reimann, Computer simulation of packing structure in pebble beds, Fusion Eng. Des. 85 (2010) 1782–1787.
[38] X. Yang, N. Gui, J. Tu, et al., 3D DEM simulation and analysis of void fraction distribution in a pebble bed high temperature reactor, Nucl. Eng. Des. 270 (2014) 404–411.
[39] L. Chen, Y. Chen, K. Huang, et al., Investigation of the packing structure of pebble beds by DEM for CFETR WCCB, J. Nucl. Sci. Technol. 53 (6) (2016) 803–808.
[40] C. Kloss, C. Goniva, A. Hager, et al., Models, algorithms and validation for open-source DEM and CFD-DEM, Progress Comput. Fluid Dyn. Int. J. 12 (2/3) (2012) 140–152.
[41] LIGGGHTS(R)-PUBLIC Documentation, Version 3. X. http://www.liggghts.com.
[42] J.V. Lew, A. Ying, M. Abdou, A discrete element method study on the evolution of thermo-mechanics of a pebble bed experiencing pebble failure, Fusion Eng. Des. 89 (2014) 1151–1157.
[43] W. Dienst, H. Zimmermann, Investigation of the mechanical-properties of ceramic breeder materials, J. Nucl. Mater. 155 (1988) 476–479.
[44] H. Zimmermann, Mechanische Eigenschaften von Lithiumsilikaten für Fusionsreaktor-Brutblankets. Technical Report, KfK 4528, Kernforschungs-zentrum Karlsruhe, 1989.
[45] G. Schumacher, M.D. Donne, S. Dorner, Properties of lithium orthosilicate spheres, J. Nucl. Mater. 155–157 (1998) 451–454.
[46] N. Zaccari, D. Aquaro, Mechanical characterization of Li_2TiO_3 and Li_4SiO_4 pebble beds: experimental determination of the material properties and of the pebble bed effective values, Fusion Eng. Des. 82 (2007) 2375–2382.
[47] Y. Gan, M. Kamlah, Discrete element modelling of pebble beds: with application to uniaxial compression tests of ceramic breeder pebble beds, J. Mech. Phys. Solids 58 (2010) 129–144.
[48] G.E. Mueller, Numerical simulation of packed beds with monosized spheres in cylindrical containers, Powder Technol. 92 (1997) 179–183 38.
[49] P. Langston, A.R. Kennedy, Discrete element modelling of the packing of spheres and its application to the structure of porous metals made by infiltration of packed beds of NaCl beads, Powder Technol. 268 (2014) 210–218.
[50] A.D. Klerk, Voidage variation in packed beds at small column to particle diameter ratio, AIChE J. 49 (8) (2003) 2022–2029.
[51] Utkarsh Ayachit, The ParaView Guide: A Parallel Visualization Application, Kitware, 2015 ISBN 978-1930934306.
[52] G.E. Mueller, Radial porosity in packed beds of spheres, Powder Technol. 203 (2010) 626–633.
[53] A.H.W. Ngan, On distribution of contact forces in random granular packings, Physica A 339 (2004) 207–227.